JGISE

Journal of Geospatial Information Science and Engineering

Coseismic Displacement Accumulation Between 1996 and 2019 Using A Global Empirical Law on Indonesia Continuously Operating Reference Station (InaCORS)

Cecep Pratama[1*], Febrian Fitryanik Susanta[1], Ridho Ilahi[2], Alian Fathira Khomaini[3], Hadi Wijaya Kusuma Abdillah[3]

[1] *Department of Geodetic Engineering, Faculty of Engineering, Universitas Gadjah Mada, Indonesia*
[2] *Graduate School of Geomatics Engineering, Faculty of Engineering, Universitas Gadjah Mada, Indonesia*
[3] *Graduate School of Geodetic Engineering, Faculty of Engineering, Universitas Gadjah Mada, Indonesia*

Corresponding Author:
Cecep Pratama
Email: *cecep.pratama@ugm.ac.id*

ABSTRACT. *Indonesia archipelago is one of the most populated country with active and complex tectonic zone in the world. Plate boundaries were assembled by four major plate which made the region not only vulnerable to earth-hazard but also prone to semi-dynamic reference frame. However, influence of transient deformation such as coseismic displacement due to large amount of small to intermediate earthquakes (< Mw 6) on the geodetic networks is remain poorly understood. Geospatial Information Agency occupied permanent and continuous GPS networks since 1996 but rapidly increase in 2010. Based on simulated empirical law of coseismic crustal deformation, we estimate the cumulative displacement due to coseismic step on Indonesia Continuous Operating Reference Stations (InaCORS). We utilize the position of the observation network and earthquake hypocentral with estimated moment magnitude. Our result suggesting small to intermediate earthquakes are indispensable for estimating secular motion and potentially contribute the cumulative offset associated with the transient postseismic deformation.*

1. Introduction

Indonesia has been a high seismicity zone lies on the pacific ring of fire. Large to great damaging earthquake occurred almost every year from 2004 to 2014 including the deadliest and tsunamigenic 2004 Mw 9.1 Sumatra-Andaman earthquake (Lay, 2015). In addition, a ten thousands of small to intermediate size of earthquake may give an indispensable accumulated strain. Those earthquakes occurrence made Indonesia region as active and complex tectonic zone suggesting a semi dynamic geodetic datum was necessary to be implemented as national reference system (Abidin et al., 2016). On the other hand, assessment of earthquake potential due to megathrust and shallow rupture required interplate coupling and intraplate locking depth, respectively. Those coupling and locking features are able to identified using secular motion in which the transient deformation such as coseismic and postseismic deformation has been removed. The coseismic offset and postseismic accumulation deformation might be shifting the secular motion prediction. Thus, the physical analysis of the earthquake cycle or definition of semi dynamic geodetic datum will be bias.

To improve both semi dynamic geodetic datum and secular deformation, previous studies proposed the coseismic model (Susilo et al., 2017). However, that studies only provide four major event > M8 class earthquake since it took physical modeling which need prior information of a complex earthquake. Other unmodeled large to great earthquake may change the displacement significantly. On the oher hand, the effect of other small and intermediate earthquake remain poorly understood.

In this study, we evaluate rough but fast estimation of the coseismic displacement accumulation on the permanent station of GPS data so called as Indonesia Continuously Operating Reference System (InaCORS). We evaluate all occurred earthquake between 1996 to 2019 based on global earthquake catalogue using simulated global

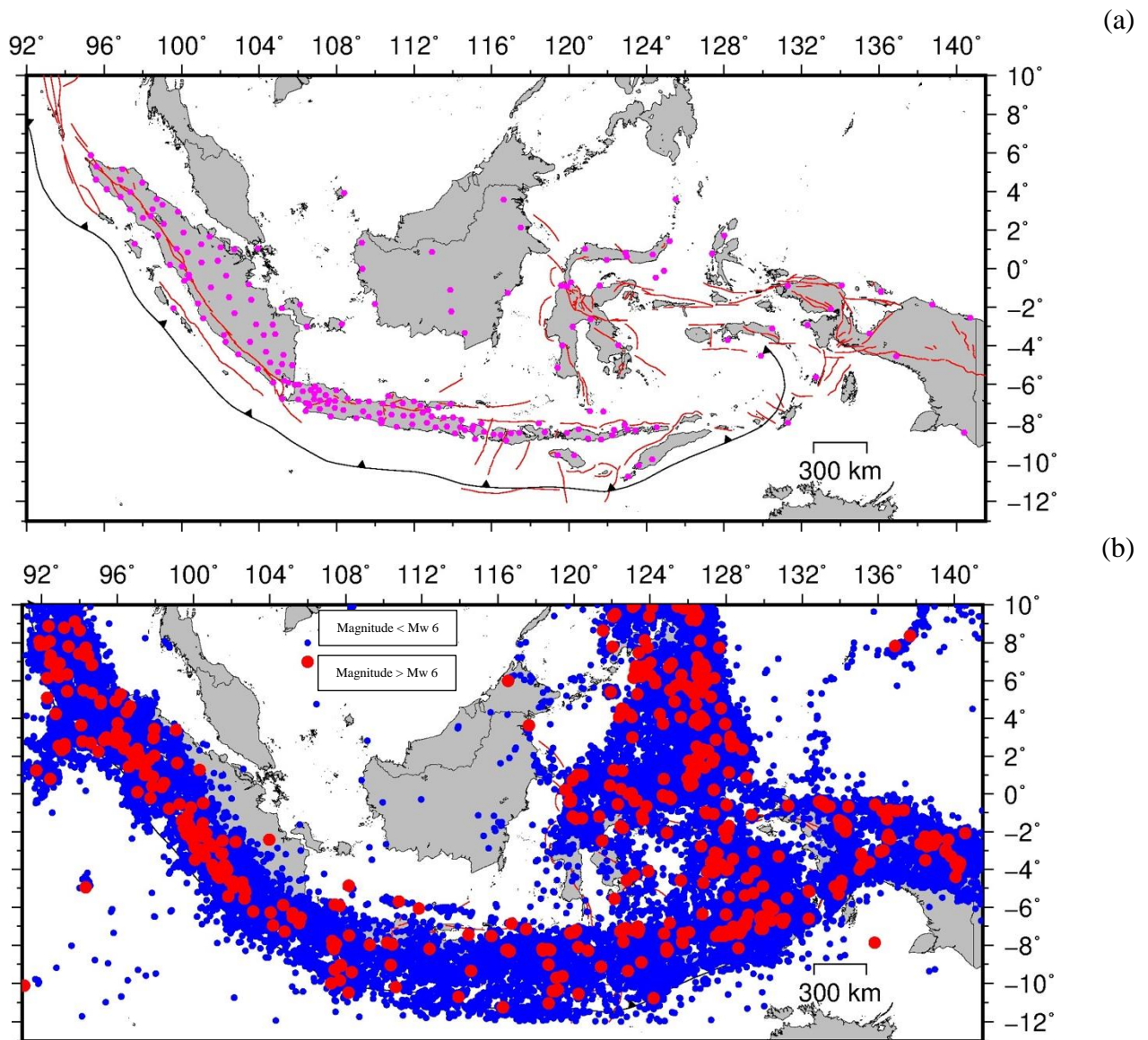empirical law of coseismic crustal deformation (Okada, 1995).

Figure 1 Red lines indicate onland fault trace while black triangle line denotes Sunda trench (a) Magenta hexagonal denotes Indonesia CORS distribution and (b) Indonesia seismicity between 1996 and 2019.

2. Data and Methods

2.1. Data

We utilized thousands of earthquake occurrence around Indonesia to estimate surface offset due to coseismic displacement on Indonesia permanent GPS networks. The permanent GPS networks, which known as Indonesia Continuously Operating Reference Stations (InaCORS), maintained by Geospatial Information Agency, Indonesia (e.g. Susilo et al., 2018). Nowadays, the agency are maintaining hundreds of GPS sites online through https://srgi.big.go.id website. In this regard, 202 sites are accessible online and being analyzed (Figure 1a).

The earthquake events based on the United States of Geological Survey (USGS) catalogue. The earthquake magnitudes are ranging between M2 (Magnitude 2) and M9 class (Figure 1b). We collected 59224 earthquakes located between 85^0 to 145^0 Longitude and -12^0 to 12^0 Latitude during January 1st, 1996 to October 31st, 2019 (Figure 2). Since our main objective is to obtain rough accumulation of thousands coseismic displacement on the permanent GPS sites, we only consider site-to-source distance based on estimated hypocenter location and magnitude moment (Mw) data. Therefore, we do not consider earthquake mechanism whether it was thrust, strike slip or normal faulting.

The earthquake catalogue resulting different magnitude scale, not only the magnitude moment (Mw) scale but also

surface wave magnitude (Ms) and body wave magnitude (mb) scale. In order to obtain homogeneous scale, we convert Ms and mb to Mw scale using empirical global relationship (Scordilis, 2006).
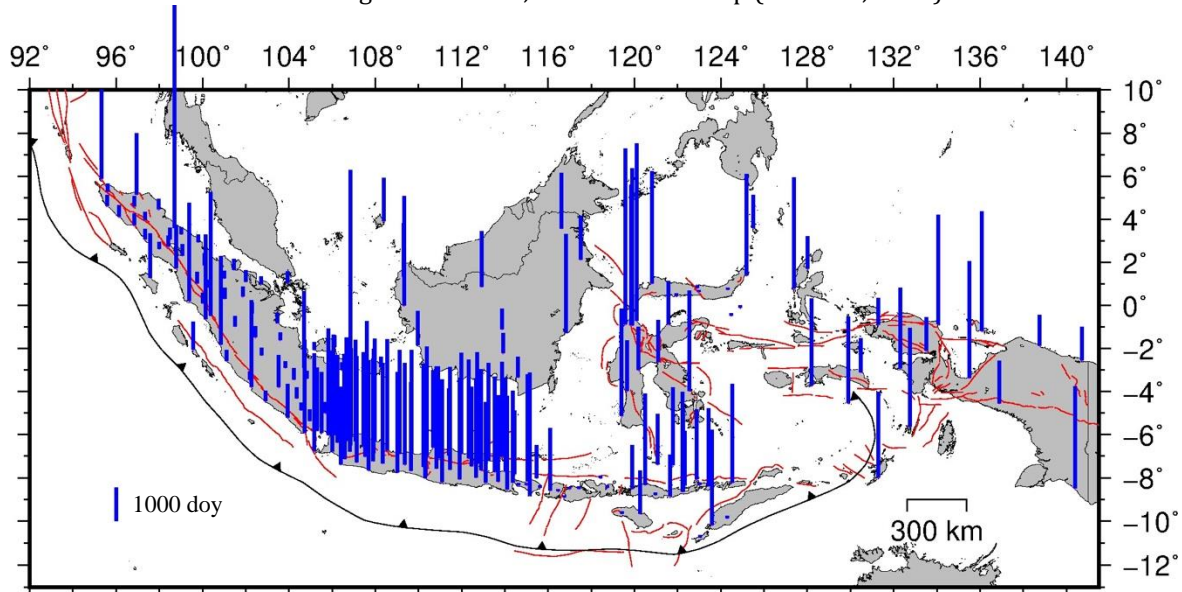

Figure 2 Number of available epoch of 202 GPS sites. Fault trace and trench line description same as Figure 1.

2.2. Methods

We estimate the maximum $U_{maximum}$ and the expected average $U_{average}$ of coseismic displacement based on empirical law of crustal deformation due to global earthquake catalogue (Okada, 1995) as follows

$$U_{maximum} = 1.5M_w - 2\log R - 6.0 \qquad (1)$$

where

$$U_{average} = 0.25U_{maximum} \qquad (2)$$

The static displacement on the GPS location was being calculated as a function of earthquake magnitude *Mw* and site-to-source hypocentral distance *R*. The empirical law derived from a million seismic sources and its observed displacement assuming a point double couple. In fact, the earthquake rupture would have finite dimension and specific mechanism within heterogeneous slip distribution. The near-field geodetic observation network are able to image the slip distribution due to large earthquake (e.g. Hashima et al., 2016; Hines & Hetland, 2016; Konca et al., 2007; Pratama et al., 2018). In that sense, we may find the coseismic estimation due to large earthquake within deviation range from maximum to 1/10 of expected average displacement especially on the near-field observation networks (Okada, 1995).

3. Result dan Discussion

We estimate the coseismic displacement on the 202 site of InaCORS using two criterion. First, the estimated displacement based on earthquake magnitude bigger than

Mw 6 which is significant but rare occurred event. Second, the estimated displacement based on all collected event from Mw 2 to Mw 9.1. The estimated displacements accumulation were summarized in the Table 1. Note that the coseismic accumulation counted after the stations built. Since BAKO and SAMP are the earliest sites was built with the observation period almost one and half decade (Figure 2). BAKO and SAMP sites shows significant displacement from 1997 to 2019 and record most of the large earthquake between 2004 to 2016 (Figure 3). SAMP site record more than 1 meter since the site was very near during the megathrust Mw 9.1 Sumatra-Andaman earthquake. Another significant displacement occurred around Palu Fault such as P14P and PALP sites. Those sites were built recently, but the 2018 Mw 7.4 earthquake struck distance was very short.

According to our calculation, earthquake with M6 to M9 contribute almost 71% cumulative coseismic displacement on GPS sites in average. Thus, another 29% contributed by M2 to M6 earthquake which is hard to be ignored. As shown in the Figure 4, we clearly obtained up to 3.11 cm cumulative displacement for magnitude moment 2 to 6. Thus, assessment of small to intermediate earthquake should be taken on secular motion estimation. The small to intermediate earthquake contribute large offset in Sumatra, West Java and Palu. Since many large earthquakes occurred in that region, we might relate the small to intermediate earthquake to aftershock sequence due to postseismic deformation (Perfettini and Avouac, 2004). The cumulative offset from postseismic deformation due to large earthquake may continuing since its process could be lasting in a several decades (Suito and Freymueller, 2009). Therefore, to obtain the more precise secular motion, we should take into account the contribution of postseismic deformation.
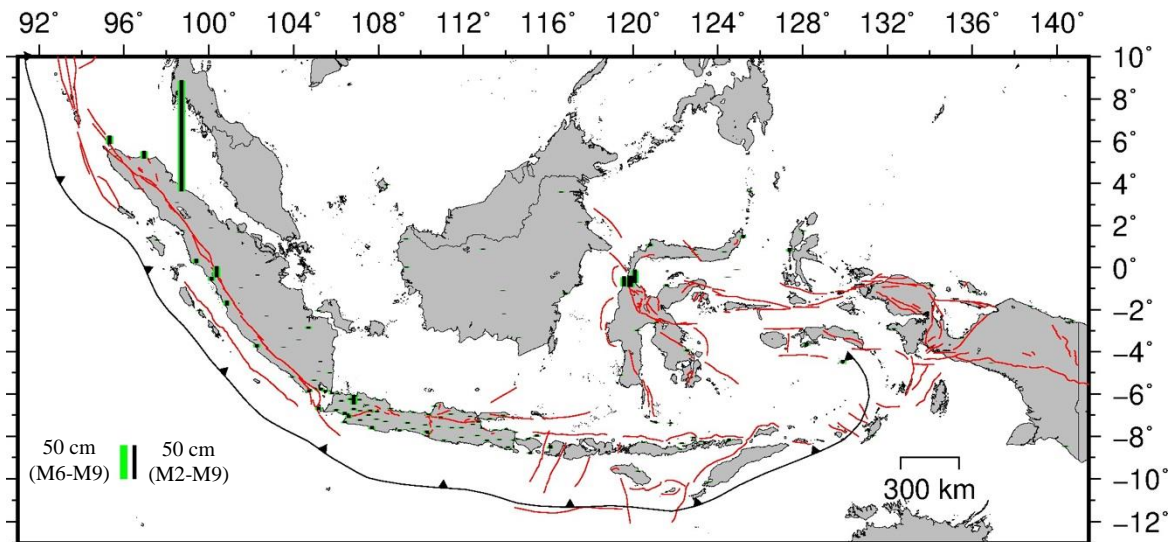
239

Figure 3 The cumulative displacement due to earthquake with all magnitude (black) and large magnitude Mw 6 to Mw 9 (green). Fault trace and trench line description same as Figure 1.
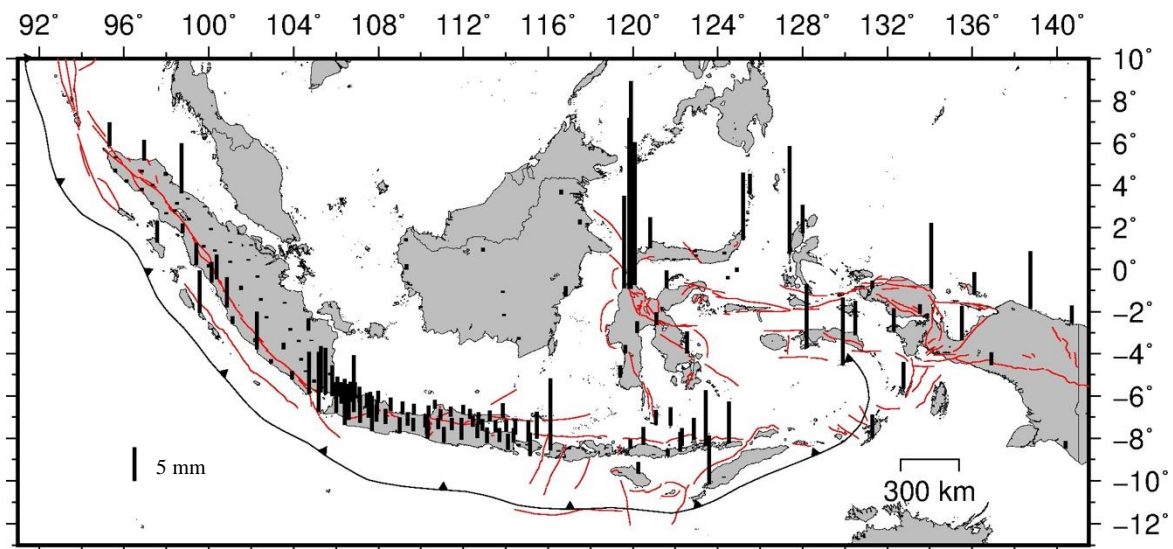
Figure 4 The cumulative displacement based on earthquake with Mw 2 to Mw 6. Fault trace and trench line description same as Figure 1.

Table 1 Detailed site profile and its expected coseismic displacement accumulation during January 1st, 1996 to October 31, 2019 based on two magnitude classification

Site Name	Lat. (°)	Lon. (°)	Starting Period	Disp.* M6-M9 (cm)	Disp.** M2-M9 (cm)	Stasiun	Lat. (°)	Lon. (°)	Starting Period	Disp. M6-M9 (cm)	Disp. M2-M9 (cm)
BAK1	-6,49	106,85	2007-08-23	4,61	4,98	CNAT	3,94	108,39	2015-12-14	0,11	0,14
BAKO	-6,49	106,85	1996-03-08	12,75	13,51	CNAU	3,59	116,62	2014-11-10	0,33	0,40
BANI	-4,52	129,90	2008-07-04	3,08	4,08	CNDE	-8,84	121,65	2015-12-06	0,26	0,36
CAGM	-3,44	102,18	2019-01-01	0,03	0,08	CNEG	-8,36	114,62	2019-06-21	0,02	0,04
CAIR	0,21	99,39	2010-08-22	5,68	6,02	CNGA	-7,60	111,91	2010-12-10	0,71	0,89
CALI	-3,01	106,46	2019-01-01	0,03	0,04	CNYU	-8,21	114,38	2010-12-08	0,86	1,08
CALO	0,63	122,98	2019-06-27	0,11	0,13	CPAC	-8,20	111,10	2010-12-06	0,73	0,96
CAMB	-3,70	128,18	2010-10-18	2,57	3,52	CPAI	-7,72	113,53	2010-12-04	0,75	0,92

240

Site Name	Lat. (°)	Lon. (°)	Starting Period	Disp.* M6-M9 (cm)	Disp.** M2-M9 (cm)	Stasiun	Lat. (°)	Lon. (°)	Starting Period	Disp. M6-M9 (cm)	Disp. M2-M9 (cm)
CAMP	-0,87	121,58	2015-12-07	1,57	1,83	CPAL	-3,01	120,19	2015-12-05	0,76	0,93
CANA	-4,45	102,92	2018-08-28	0,06	0,12	CPAR	-0,63	100,13	2010-08-19	5,24	5,55
CANG	-7,02	107,52	2010-11-26	1,10	1,36	CPAS	-7,65	112,90	2010-12-03	0,71	0,89
CBAG	-8,44	115,61	2019-06-24	0,01	0,03	CPBI	-8,01	115,47	2008-06-30	1,67	2,07
CBAK	-9,64	119,41	2019-06-28	0,02	0,03	CPBL	-7,39	109,36	2010-11-14	0,92	1,11
CBAL	-1,26	116,84	2010-01-10	1,14	1,28	CPBM	-3,43	104,24	2018-08-08	0,06	0,09
CBAS	1,36	109,30	2014-11-11	0,14	0,18	CPBR	-8,35	122,32	2009-11-08	0,70	0,97
CBDA	5,30	95,61	2019-01-01	0,01	0,03	CPES	-8,53	114,11	2010-12-22	0,80	1,03
CBIK	-1,19	136,09	2009-06-14	1,46	1,79	CPKL	-6,89	109,67	2010-11-14	0,86	1,02
CBIM	-8,46	118,75	2019-06-24	0,02	0,03	CPKY	-2,21	113,92	2017-10-24	0,16	0,19
CBIT	1,44	125,19	2010-01-05	2,25	3,24	CPMK	-7,66	107,69	2007-12-16	3,42	3,94
CBJM	-3,33	114,61	2017-10-25	0,19	0,22	CPOH	0,47	121,94	2019-07-03	0,07	0,09
CBJW	-8,79	120,98	2019-06-25	0,02	0,03	CPON	0,00	109,33	2010-01-22	1,19	1,26
CBJY	-4,95	105,18	2018-07-27	0,12	0,14	CPPR	0,86	100,30	2018-11-21	0,01	0,04
CBKJ	3,99	97,34	2019-01-01	0,01	0,03	CPRE	-3,98	119,65	2015-05-05	0,49	0,62
CBKL	-3,80	102,27	2010-08-11	4,34	4,91	CPRI	-5,36	104,97	2018-07-19	0,15	0,19
CBKN	0,34	101,02	2018-08-22	0,03	0,05	CPSM	0,12	100,01	2018-08-29	0,03	0,06
CBKT	-0,31	100,37	2009-08-29	10,90	11,22	CPSR	-6,01	105,83	2008-02-21	2,00	2,46
CBLA	-3,10	130,49	2016-09-23	0,39	0,89	CPTN	-6,96	106,41	2007-12-17	2,08	2,64
CBLG	2,33	99,07	2018-07-29	0,02	0,06	CPTS	-8,01	110,30	2015-06-12	0,18	0,29
CBLR	-6,97	111,41	2010-12-11	0,74	0,88	CPTU	-6,99	106,55	2010-12-22	1,18	1,56
CBLT	-2,87	108,27	2018-08-25	0,06	0,07	CPUT	0,88	112,92	2014-11-11	0,20	0,24
CBOH	4,14	96,13	2018-07-22	0,02	0,06	CPWD	-7,10	110,91	2010-12-11	0,76	0,91
CBOM	0,74	124,31	2019-07-07	0,10	0,13	CPWK	-6,55	107,44	2011-01-11	1,07	1,28
CBON	-7,38	121,08	2009-11-27	0,75	0,98	CRAU	2,15	117,50	2015-12-04	0,49	0,56
CBPI	3,74	96,84	2018-07-26	0,02	0,06	CREO	-8,31	120,49	2009-11-27	0,75	1,02
CBRN	-7,84	114,44	2008-06-24	1,19	1,43	CRKS	-6,36	106,25	2010-12-16	1,22	1,53
CBTI	-2,10	133,52	2016-09-24	0,21	0,35	CROL	-6,31	107,98	2010-12-11	1,01	1,18
CBTL	-7,89	110,34	2010-11-20	0,79	1,02	CRTE	-10,73	123,05	2019-07-01	0,02	0,03
CBTM	1,07	103,93	2018-08-14	0,03	0,05	CRUT	-7,22	107,90	2010-12-03	1,12	1,37
CBTU	-6,31	107,10	2010-08-05	1,27	1,51	CSAB	5,89	95,32	2011-09-17	10,91	11,26
CBUA	-0,11	124,90	2019-06-27	0,36	0,42	CSAP	1,12	102,01	2018-07-27	0,03	0,05
CCIR	-6,72	108,56	2010-01-07	1,21	1,41	CSAU	-7,98	131,30	2010-10-24	0,80	1,15
CCLP	-7,74	109,01	2010-11-16	0,99	1,22	CSBA	-8,91	116,75	2019-07-02	0,01	0,03
CDAI	-8,07	122,87	2009-11-10	0,73	1,05	CSBE	-8,50	117,43	2019-06-26	0,02	0,03
CDNP	-8,82	115,15	2008-05-15	1,29	1,63	CSBH	1,05	99,74	2018-07-19	0,03	0,06
CDOM	-8,01	118,43	2019-06-24	0,02	0,03	CSBK	-5,90	105,51	2008-02-21	2,10	2,78
CDRI	1,27	101,01	2019-01-01	0,01	0,03	CSBL	2,74	98,41	2018-08-02	0,02	0,05

Site Name	Lat. (°)	Lon. (°)	Starting Period	Disp.* M6-M9 (cm)	Disp.** M2-M9 (cm)	Stasiun	Lat. (°)	Lon. (°)	Starting Period	Disp. M6-M9 (cm)	Disp. M2-M9 (cm)
CDUM	1,68	101,45	2018-08-14	0,03	0,05	CSBS	2,64	98,00	2019-01-01	0,01	0,03
CELO	-8,62	116,47	2019-07-03	0,01	0,03	CSBY	-7,33	112,72	2010-01-08	0,85	1,02
CFAK	-2,92	132,30	2010-10-24	0,75	1,09	CSDH	-0,97	101,51	2018-08-01	0,04	0,10
CGMS	-1,10	113,87	2017-10-28	0,16	0,19	CSEK	-2,89	103,84	2018-08-14	0,05	0,08
CGON	-6,02	106,05	2010-12-22	1,24	1,53	CSEL	-1,80	100,84	2010-08-14	6,59	7,04
CGUT	0,84	122,92	2019-07-02	0,10	0,12	CSEM	-6,99	110,38	2010-01-13	0,97	1,13
CJBI	-1,61	103,59	2018-11-21	0,03	0,04	CSIB	1,74	98,78	2015-12-12	0,22	0,36
CJEM	-8,17	113,69	2010-12-21	0,75	0,96	CSIT	-7,70	114,01	2010-12-06	0,84	1,02
CJKT	-6,11	106,88	2010-07-07	1,33	1,56	CSLI	-1,86	106,11	2018-08-17	0,05	0,07
CJPR	-6,60	110,67	2010-11-24	0,78	0,91	CSLO	-7,57	110,83	2010-11-22	0,76	0,93
CJUR	-6,82	107,14	2011-03-13	1,10	1,36	CSMI	-1,85	138,75	2016-09-18	0,45	1,30
CJYP	-2,54	140,70	2016-09-29	0,34	0,59	CSMN	-7,02	113,88	2010-11-29	0,78	0,99
CKAG	-3,39	104,83	2019-01-01	0,04	0,06	CSMP	-7,20	113,25	2010-11-30	0,73	0,88
CKAL	-8,21	124,52	2009-11-27	1,37	1,98	CSOE	-9,86	124,29	2019-06-21	0,07	0,08
CKBJ	3,10	98,50	2018-08-07	0,02	0,05	CSOQ	-0,88	131,28	2017-03-16	0,30	0,41
CKBM	-7,67	109,65	2010-12-27	0,89	1,08	CSRJ	-8,15	115,06	2008-07-21	1,31	1,62
CKEF	-0,45	124,48	2019-06-24	0,23	0,27	CSRL	-2,30	102,72	2019-01-01	0,03	0,05
CKEN	-3,96	122,54	2010-09-22	0,96	1,28	CSUM	-6,86	107,92	2010-11-30	1,07	1,28
CKMN	-4,87	104,57	2019-01-01	0,09	0,11	CSWA	-8,52	116,99	2019-06-29	0,02	0,03
CKPI	1,89	100,09	2018-07-24	0,03	0,05	CTAB	-8,33	115,00	2019-06-29	0,01	0,03
CKRC	0,42	101,86	2018-08-09	0,03	0,05	CTAK	4,62	96,85	2018-08-08	0,02	0,05
CKRI	-5,20	103,93	2016-10-01	0,15	0,27	CTAN	-7,27	107,12	2010-12-21	1,13	1,46
CKTF	3,09	97,33	2018-07-19	0,02	0,06	CTBL	1,73	128,01	2016-09-30	0,67	1,09
CKTK	-0,81	103,47	2018-07-19	0,04	0,06	CTBN	-6,87	111,99	2010-11-26	0,73	0,86
CKTP	-1,83	109,98	2016-09-18	0,11	0,14	CTBT	3,34	99,00	2019-01-01	0,01	0,02
CKUP	-10,17	123,60	2009-11-14	0,66	1,39	CTCN	-5,91	104,73	2008-02-21	2,35	2,97
CLAN	4,63	95,58	2018-07-31	0,02	0,06	CTER	0,79	127,38	2009-12-29	2,69	4,29
CLBG	-6,82	107,62	2008-01-08	2,02	2,33	CTGL	-6,87	109,14	2010-11-12	0,92	1,11
CLBJ	-8,50	119,88	2015-12-02	0,36	0,50	CTGR	-6,29	106,66	2009-07-13	1,79	2,09
CLDO	-6,77	106,83	2007-11-06	2,05	2,45	CTHN	3,61	125,50	2016-09-16	0,61	0,90
CLGI	-5,81	105,30	2008-02-21	2,15	2,83	CTIM	-4,55	136,89	2015-12-15	0,23	0,42
CLHT	-3,80	103,53	2016-10-06	0,11	0,20	CTJB	2,96	99,81	2019-01-01	0,01	0,02
CLMG	-7,09	112,33	2010-12-10	0,72	0,86	CTOA	-7,41	121,77	2009-11-27	0,74	1,01
CLSA	4,47	97,97	2018-08-15	0,02	0,06	CTOL	1,03	120,82	2009-10-28	2,34	2,80
CLUM	-8,21	113,11	2010-12-17	0,71	0,93	CTUL	-8,07	111,91	2010-12-13	0,71	0,91
CLWB	-8,37	123,42	2009-11-27	0,74	1,57	CTVI	-7,12	106,60	2007-11-24	2,22	2,75
CMAG	-7,61	111,45	2010-12-08	0,73	0,90	CUAL	-5,63	132,75	2010-10-30	0,75	1,14
CMAK	-5,13	119,41	2009-12-31	0,89	1,07	CUJG	-7,38	106,41	2007-12-05	2,24	2,86

Site Name	Lat. (°)	Lon. (°)	Starting Period	Disp.* M6-M9 (cm)	Disp.** M2-M9 (cm)	Stasiun	Lat. (°)	Lon. (°)	Starting Period	Disp. M6-M9 (cm)	Disp. M2-M9 (cm)
CMAN	-0,86	134,07	2009-06-07	1,21	2,18	CUJK	-6,75	105,18	2008-04-05	2,71	3,60
CMAT	-8,58	116,10	2013-12-04	3,29	4,37	CUKA	-8,33	123,00	2019-06-23	0,07	0,08
CMEN	-4,47	105,25	2018-07-31	0,09	0,12	CUKE	-8,49	140,39	2010-09-26	0,63	0,74
CMGL	-7,48	110,22	2010-11-19	0,81	1,00	CWAI	-9,65	120,26	2015-12-08	0,37	0,54
CMIS	-7,33	108,34	2010-12-06	1,09	1,32	CWJP	-5,01	105,71	2018-07-22	0,11	0,14
CMJT	-7,47	112,44	2010-12-01	0,71	0,87	JOGS	-7,82	110,29	2007-08-23	2,19	2,47
CMLG	-7,98	112,66	2010-12-16	0,70	0,90	LHMI	5,18	96,95	2010-01-19	10,69	11,00
CMLI	-2,63	121,10	2015-12-06	0,89	1,07	MMRI	-8,64	122,24	2008-09-17	0,83	1,13
CMLP	-6,78	106,02	2010-12-19	1,31	1,76	NIAS	1,30	97,58	2015-04-05	0,27	0,59
CMOL	-0,36	102,29	2018-08-06	0,03	0,06	P14P	-0,91	119,84	2002-10-18	13,04	15,59
CMRE	-8,63	122,22	2009-11-04	0,70	0,96	PALE	-2,90	104,70	2009-02-23	2,43	2,61
CMRT	1,01	102,71	2019-01-01	0,02	0,03	PALP	-0,92	119,91	2002-06-05	13,00	16,11
CMTB	-1,48	102,44	2018-07-22	0,04	0,08	PANJ	-0,47	100,38	2011-01-01	3,75	4,01
CMTK	-2,05	105,17	2019-01-01	0,03	0,04	S1PO	-2,05	99,58	2013-05-09	0,58	1,21
CMTP	-4,32	104,35	2018-08-05	0,08	0,11	SAMP	3,62	98,71	1997-11-16	165,78	166,53
CMUK	-2,57	101,11	2018-08-22	0,05	0,16	TOBP	-0,71	120,09	2000-10-08	17,26	19,39
CNAB	-3,37	135,51	2009-06-11	1,39	1,90	WATP	-0,87	119,59	2000-10-09	12,35	13,72

* Displacement due to M6 to M9   ** Displacement due to M2 to M9

4. Conclusions

We estimate the cumulative coseismic displacement on distributed InaCORS based on earthquake catalogue between 1996 and 2019. The largest offset contribution on the GPS sites are influenced by large earthquake with magnitude > Mw 6 in which almost 90% cumulative displacement covered. Although the contribution of earthquake < Mw 6 is small, several region may reflect aftershock sequence which is related with the postseismic deformation. Therefore, large number of small events could potentially bias the secular motion. In further studies, we intend to investigate the model of the cumulative offset from postseismic deformation to enhance InaCORS accuracy.

5. Conflict of Interest Statement

The authors declare no competing interest.

6. References

Abidin, H. Z., Susilo, S., Meilano, I., Subarya, C., Prijatna, K., Syafi'i, M. A., Hendrayana, E., Effendi, J., & Sukmayadi, D. (2016). On the development and implementation of a semi-dynamic datum for Indonesia. In *International Association of Geodesy Symposia*.

https://doi.org/10.1007/1345_2015_83

Hashima, A., Becker, T. W., Freed, A. M., Sato, H., & Okaya, D. A. (2016). Coseismic deformation due to the 2011 Tohoku-oki earthquake: influence of 3-D elastic structure around Japan. *Earth, Planets and Space*, *68*(1), 159. https://doi.org/10.1186/s40623-016-0535-9

Hines, T. T., & Hetland, E. A. (2016). Rapid and simultaneous estimation of fault slip and heterogeneous lithospheric viscosity from post-seismic deformation. *Geophysical Journal International*, *204*(1), 569–582. https://doi.org/10.1093/gji/ggv477

Konca, A. O., Hjorleifsdottir, V., Song, T. R. A., Avouac, J. P., Helmberger, D. V., Ji, C., Sieh, K., Briggs, R., & Meltzner, A. (2007). Rupture kinematics of the 2005 Mw 8.6 m Nias-Simeulue earthquake from the joint inversion of seismic and geodetic data. *Bulletin of the Seismological Society of America*, *97*(1 A SUPPL.). https://doi.org/10.1785/0120050632

Lay, T. (2015). The surge of great earthquakes from 2004 to 2014. *Earth and Planetary Science Letters*. https://doi.org/10.1016/j.epsl.2014.10.047

Okada, Y. (1995). Simulated Empirical Law of Coseismic Crustal Deformation. *Journal of Physics of the Earth*, *43*, 697–713. https://doi.org/10.4294/jpe1952.43.697

Perfettini, H. (2004). Postseismic relaxation driven by brittle creep: A possible mechanism to reconcile

geodetic measurements and the decay rate of aftershocks, application to the Chi-Chi earthquake, Taiwan. *Journal of Geophysical Research*, *109*(B2), 1–15. https://doi.org/10.1029/2003JB002488

Pratama, C., Ito, T., Tabei, T., Kimata, F., Gunawan, E., Ohta, Y., Yamashina, T., Nurdin, I., Sugiyanto, D., Muksin, U., Ismail, N., & Meilano, I. (2018). Evaluation of the 2012 Indian Ocean coseismic fault model in 3-D heterogeneous structure based on vertical and horizontal GNSS observation. In *AIP Conference Proceedings*. https://doi.org/10.1063/1.5047296

Scordilis, E. M. (2006). Empirical global relations converting MS and mb to moment magnitude. *Journal of Seismology*. https://doi.org/10.1007/s10950-006-9012-4

Suito, H., & Freymueller, J. T. (2009). A viscoelastic and afterslip postseismic deformation model for the 1964 Alaska earthquake. *Journal of Geophysical Research: Solid Earth*, *114*(11). https://doi.org/10.1029/2008JB005954

Susilo, Abidin, H. Z., Meilano, I., Sapiie, B., Gunawan, E., Wijarnto, A. B., & Efendi, J. (2017). Preliminary co-sesimic deformation model for Indonesia geospatial reference system 2013. In *AIP Conference Proceedings*. https://doi.org/10.1063/1.4987073

Susilo, Meilano, I., Abidin, H. Z., Sarsito, D. A., Sapiie, B., & Efendi, J. (2018). Geodetic strain to study the deformation model of Indonesian semi dynamic datum 2013. In *AIP Conference Proceedings*. https://doi.org/10.1063/1.5047387